

Contents

1	Introduction	1
2	Theoretical Background	1
2.1	Law of Radioactive Decay	1
2.2	Different Types of Decay	1
2.2.1	α - decay	1
2.2.2	β^- - decay	2
2.2.3	Electron capture	2
2.3	γ decay	3
2.4	Internal Conversion	3
2.5	Inorganic Scintillator:	3
2.6	Used Isotopes of this Experiment and their Decays	4
2.6.1	Americium or ^{241}Am	4
2.6.2	Cobalt or ^{57}Co	4
2.7	Delayed Coincidence Method	5
3	Experimental Setup	6
3.1	NIM-Modules	6
3.1.1	Main Amplifier (MA)	6
3.1.2	Multi Channel Analyzer (MCA)	6
3.1.3	Single Channel Analyzer (SCA)	6
3.1.4	Time Amplitude Converter (TAC)	6
3.2	Circuit setups for the different parts	7
4	Execution of the Experiment	9
5	Data Analysis	10
5.1	Energy Spectra	10
5.2	Energy Calibration	12
5.3	Time Calibration	18
5.4	Half Life of the 14.4 keV State of ^{57}Fe	19
5.4.1	SCA Windows	19
5.4.2	Delayed Coincidence Measurement	20
5.4.3	Random Coincidences	20
5.4.4	Linear Fit	20
5.4.5	Exponential Fit	22
6	Summary and Discussion of Results	24
7	Appendix	25
7.1	Calculation of Asymmetric Errors	25
7.2	Lab Notes	27
	References	30

List of Figures

1	Feynman diagram of the β^- -decay.	2
2	Feynman diagram of electron capture.	2
3	Band structure of a doped scintillation crystal [4]	3
4	The simplified decay scheme of the ^{241}Am decay	4
5	The simplified decay scheme of the ^{57}Co isotope	5
6	Photographs of the two samples. In the background of fig. 6a, the two detectors can be seen.	7
7	A block circuit diagram for the energy calibration as well as the setting of the energy windows	7
8	A block circuit diagram for the time calibration.	8
9	A block circuit diagram for the time calibration.	8
10	Two signals in comparison.	9
11	Energy spectrum of ^{241}Am as measured with the detector on the right side at different orientations of the sample	11
12	Energy spectrum of ^{241}Am as measured with the detector on the left side at different orientations of the sample	11
13	Energy spectrum of ^{57}Co as measured with the detector on the right side at different orientations of the sample	12
14	Energy spectrum of ^{57}Co as measured with the detector on the left side at different orientations of the sample	12
15	Fit of a gaussian function (eq. 8) to the single peak in the ^{241}Am spectrum	13
16	Fit of a superposition of two gaussian functions (eq. 11) to the double peak in the ^{241}Am spectrum	14
17	Fit of a gaussian function (eq. 8) to the large peak in the ^{57}Co spectrum	15
18	Fit of a gaussian function (eq. 8) to the small peak in the ^{57}Co spectrum	15
19	Fit of linear function (eq. 20) for energy calibration	16
20	Linear fit relating the MCA channels to their corresponding time difference Δt	18
21	plots of the MCA measurement with the SCA windows set on the respective ^{57}Co peaks	19
22	Plot of the delayed coincidence measurement	20
23	Linear fit (eq. 33) to $\log(N)$ of channels 23 to 90 of fig. 22.	21
24	Exponential fit (eq. 47) to the counts N of channels 23 to 90. The function with the estimated parameters is drawn as a blue line.	22
25	Exponential fit (eq. 47) to the counts N of channels 23 to 90, where the fit parameters are constrained by eq. 48. The function with the estimated parameters is drawn as a blue line.	23

List of Tables

1	Assignment of the peaks found to the Photon energies E_γ given in [1] . . .	16
2	Calculation of the energies E corresponding to the observed peaks and comparison to the literature values E_γ	17
3	Borders of the two peaks used for the delayed coincidences measurement . .	19
4	Results for the half life $T_{1/2}$ of the 14.4 keV state of ^{57}Fe and consistency with the reference value $T_{1/2} = 98$ ns	24
5	Values of the natural logarithm of the measured Counts and respective upper and lower uncertainties used for fitting.	25

1 Introduction

The experiment is about the short half lives. The aim will be to determine the life time of the ^{57}Fe 14.4 KeV state with the delayed coincidence method. To understand what is happening within the experiment, we will give short explanations of the different decays that are possible and the ones we are observing in the following section, followed by the instruments and methods used to measure the life time.

2 Theoretical Background

The formulas and the theories are taken from [1], if not cited differently.

2.1 Law of Radioactive Decay

Most elements and their isotopes are stable, but neither the less some are unstable and decay over time. This phenomenon is called radioactive decay. This process is a statistical process, where the number of atoms N over time can be described with the following relation:

$$\frac{dN}{dt} = -\lambda \cdot N \quad (1)$$

Here is λ the specific decay constant for an isotope. Through integration this results in the *Law of radioactive decay*

$$N(t) = N_0 \cdot e^{-\lambda \cdot t}, \quad (2)$$

N_0 describes the number of atoms at the time 0 ($N_0 = N(0)$). The most interesting quantity of Radioactive decay is the so called Half-life $T_{1/2}$. it indicates the time, after which half of the beginning atoms have decayed.

$$N(T_{1/2}) = \frac{N_0}{2} \iff T_{1/2} \stackrel{\tau = \frac{1}{\lambda}: \text{lifetime}}{\stackrel{\downarrow}{=} \tau \ln 2} \quad (3)$$

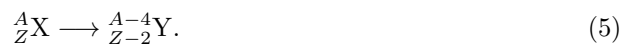
Another important quantity is the activity A which is the negative change rate in the number of atoms.

$$A = -\frac{dN}{dt} = \lambda \cdot N(t) = \frac{\ln 2}{T_{1/2}} N(t) \quad (4)$$

2.2 Different Types of Decay

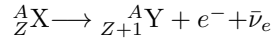
2.2.1 α - decay

A parent nucleus X decays over time into its so called daughter nucleus Y. The common notation for nuclei and their compositions is ^A_ZX where X is the element, A is the number of protons plus the number of neutrons in the nucleus and Z is the number of protons without the neutrons. An α particle consists of two protons and two neutrons and therefore a twice positively charged He nucleus (^4_2He). This kind of decay mainly occurs in heavy nuclei. The reaction Formula for the α -decay is given by:



2.2.2 β^- - decay

β^- rays consist of electrons and anti electron neutrinos.



The Weak interaction changes with a W^- -boson one down-quark into one up-quark, and therefore the neutron into a proton.

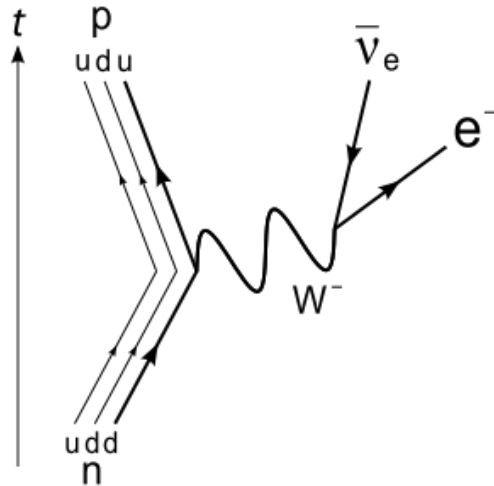


Figure 1: Feynman diagram of the β^- -decay. This picture was taken from [2]

2.2.3 Electron capture

The phenomenon of the electron capture is another way of a β^- -decay. Instead of a neutron which becomes a proton, the opposite is the case. An electron from the lower k-shell is being absorbed in the nucleus and an electron neutrino emitted. A Feynman diagram can be seen in Figure 2. The Electron capture does take place in this experiment, but it is not the one, we will be detecting.

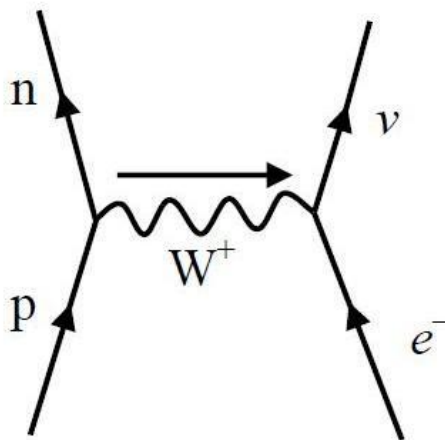


Figure 2: Feynman diagram of electron capture. This picture was taken from [3]

2.3 γ decay

In this experiment, we will only be able to detect the γ decay which takes place when an isotope decays into an excited state of the daughter isotope. When this relaxes into a lower energy state, it emits γ rays with a frequency proportional to the energy difference of those states.

2.4 Internal Conversion

Another phenomenon that can occur during the relaxation of an excited nucleus is the internal conversion, where the excess energy is not emitted as a Photon but absorbed by an Electron in the atomic shell which then has enough energy to surmount its binding energy and is emitted from the atom. The hole which is left by the emitted electron is filled by an electron from an energetically higher shell. The energy difference between the shells for its part can be emitted as X-radiation or by emission of another electron which is then called Auger electron.

2.5 Inorganic Scintillator:

An inorganic scintillator has a lattice structure. An absorbed photon causes a collective lattice excitation of the crystal. By solving the stationary Schrödinger equation for a periodic potential, one can show that the atoms in a crystalline material have got collective energy bands (cf. fig. 3).

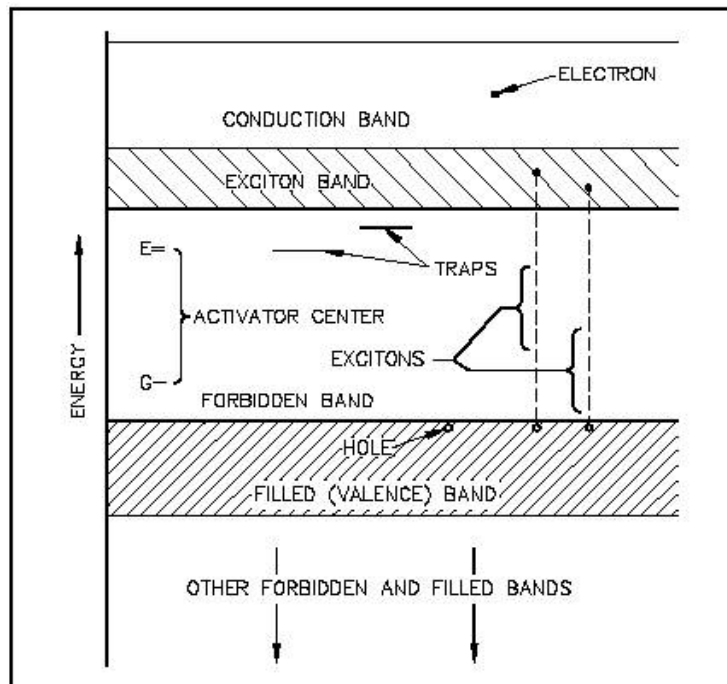


Figure 3: Band structure of a doped scintillation crystal [4]

An electron in the valence band can be excited into the conduction band where it moves freely and the crystal becomes a conductor. In the valence band there remains a hole which also moves freely through the crystal. An electron that is excited by a photon but does not absorb enough energy to reach the conduction band, is still loosely bound to the hole. This

electron-hole-pair is called an exciton and can also move freely inside the crystal. When the electrons relax into the valence band, another photon is emitted. To be able to detect this photon, it has to be made sure that it is not re-absorbed by the crystal. This is achieved by doping the crystal with activator atoms. This so called activator impurity locally deforms the conduction band and creates new energy levels. The electrons, holes and excitons move through the crystal until they reach such an impurity, where they recombine emitting a photon which hasn't got enough energy to excite a valence electron into the conduction band. Therefore these activator photons can pass through the crystal and be detected.

2.6 Used Isotopes of this Experiment and their Decays

There are two different isotopes used in this experiment, one is used for the calibration of the energy spectra, the other one shall be examined and the life time of one excited state is to be determined.

2.6.1 Americium or ^{241}Am

^{241}Am decays with α -decay into the excited state of ^{237}Np Which has an energy of 59.5 keV. By γ decay it can relax further directly to the ground state, or before that to the 33.2 keV state. This isotope is going to be used as the calibration for the energy axis later on. A simplified diagram of those decays can be seen in figure 4.

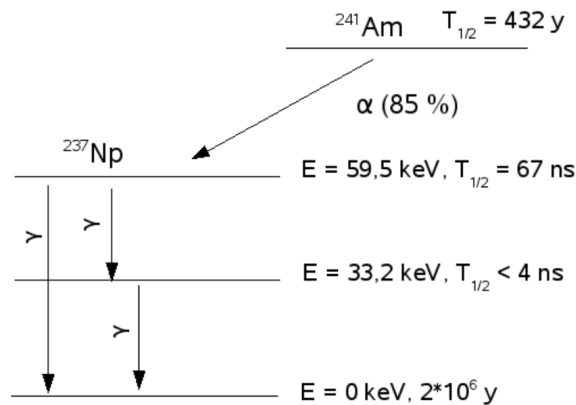


Figure 4: The simplified decay scheme of the ^{241}Am decay

2.6.2 Cobalt or ^{57}Co

The ^{57}Co isotope decays via Electron Capture into the excited state of the ^{57}Fe isotope with an energy of 136.5 keV. In 88 out of 100 cases this relaxes by emitting a γ ray to the 14.4 keV state, whose life time shall be identified. In the other 12 cases, it decays directly into the ground state. From the 14.4 keV state there are two different ways for the state to relax. One by internal conversion which we are not able to measure. The other is less likely but relaxes by γ decay. A systematic diagram can be seen in Figure 5

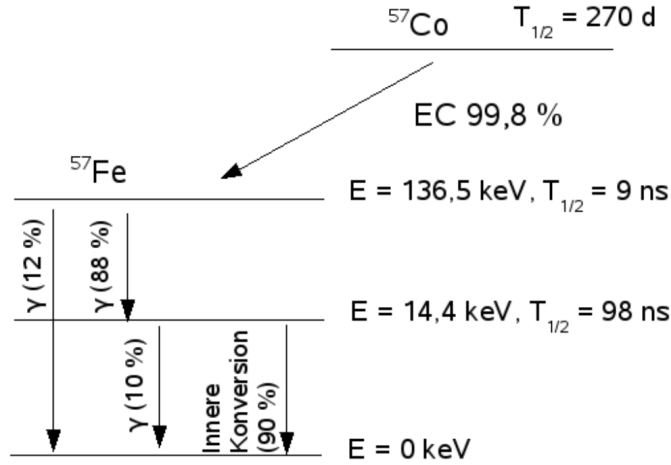


Figure 5: The simplified decay scheme of the ^{57}Co isotope

2.7 Delayed Coincidence Method

We want to measure the life time of the 14.4 keV state. The NIM modules which we use, allow us to start a measurement by one signal and stop it with another. We obtain a signal with an amplitude proportional to the time difference. The easiest way would be to use the signal from the relaxation between the 136.5 and 14.4 keV decay as the start signal and the 14.4 keV signal for the stop signal. But because the 14.4 decays with a probability of 90 % with Internal conversion, we will only stop in 1 out of ten events. Therefore the time the computer waits after receiving a start signal will cover up events which we might actually want to detect, and instead receive a stop signal by a 14.4 keV photon from another atom. The idea to measure this life time τ is to start with the 14.4 keV signal because we know that every time we detect a 14.4 signal, a signal with the energy of 122.1 keV must have been there before. What we do is, that we delay the 122.1 keV signal by a minimum of the expected life time. This means, that with a known delay we can expect the stop signal after the start signal within a certain time. The time difference between those signals will be called Δt . The inversion of start and stop signal leads to an exponential curve of the following form:

$$N(\Delta t) = N_0 \exp \left[\frac{\Delta t}{\tau} \right] \quad (6)$$

The delay t_D of the stop signal shifts the curve to the right. The shifted curve is the one measured in the experiment. Therefore, to obtain the physical decay curve, we have to consider a function

$$N(\Delta t) = N_0 \exp \left[\frac{\Delta t + t_D}{\tau} \right] \quad (7)$$

3 Experimental Setup

In the setup of this experiment, the main parts are the two inorganic scintillators, which are positioned in 180° degrees from one another with a space in between, where the samples are placed. This can be seen in Figure 6a. Also one can see the sample of the americium, where the more active side is turned upwards. In Figure 6b the cobalt sample is pictured in front of lead covered setup. The two scintillation detectors have a built-in photo multiplier (PM), which then sends the signal to an amplifier (PA) which is also built into the detector. After the pre amplification the received signal will take different routes through the NIM-modules throughout the experiment depending on the quantity measured.

3.1 NIM-Modules

3.1.1 Main Amplifier (MA)

The amplification level can be controlled by the *gain* controller (and the *coarse gain* for adjustment on a higher scale). The *Shaping Time* controller determines the shape of the output signal. Within the adjusted shaping time interval, the maximum amplitude is determined. The shaping time should be elected to be long enough to reach the maximum amplitude but short enough to reduce the dead time resulting from the delay of the output signal by the shaping time. There are two modes of the output signal: The unipolar output, which delivers a gaussian-shaped signal and the bipolar output, which delivers a dispersion curve.

3.1.2 Multi Channel Analyzer (MCA)

The multi channel analyzer measures the height of an incoming pulse by comparing it with a sawtooth voltage signal. The pulses are then distributed into an adjustable number of channels, sorting them by their height. In the experiment, after an energy calibration, the channels can be assigned with a corresponding energy each.

3.1.3 Single Channel Analyzer (SCA)

The single channel analyzer only detects incoming signals with a certain amplitude window. The amplitude window can be adjusted with a *lower level* and a *upper level* controller. In the experiment, the amplitude window is adjusted for the equipment to only detect photons within a certain energy frame. The output of the SCA is a logical rectangular signal.

3.1.4 Time Amplitude Converter (TAC)

The time amplitude converter takes two negative logic inputs and gives a signal, whose height is proportional to the time difference of those.

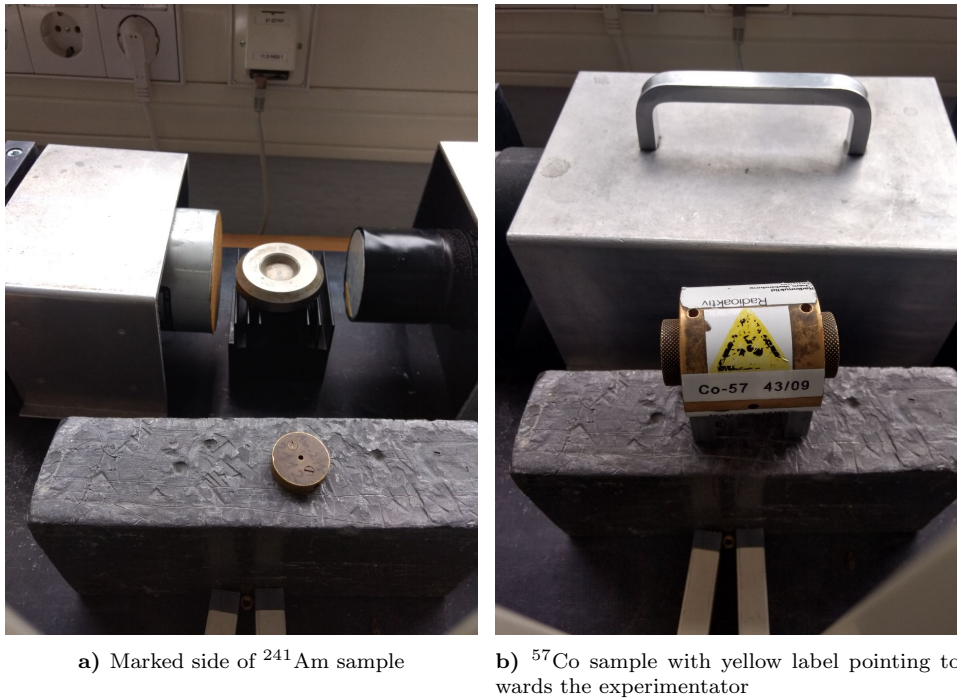


Figure 6: Photographs of the two samples. In the background of fig. 6a, the two detectors can be seen.

3.2 Circuit setups for the different parts

In the first part we use a setup, which can be seen schematically in Figure 7. It was used firstly for measuring the energy spectra of every alignment of the samples for both scintillators.

For the second part, the time calibration, we need the setup of Figure 8 where the signal from the SCA is being delayed by a certain time and the TAC gives the output signal to the MCA, which then puts the signal into the respective bin depending on its amplitude.

For the last part, the delayed coincidence measurement, the signal of the 122.1 keV signal gets delayed by three delay units, of which each one can delay a signal by up to 66 ns. the 14.4 keV signal goes straight into the TCA. From there the signal goes through the MCA to the computer. this setup can be seen in Figure 9

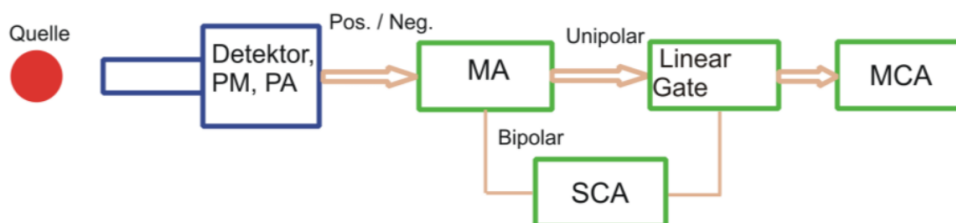


Figure 7: A block circuit diagram for the energy calibration as well as the setting of the energy windows

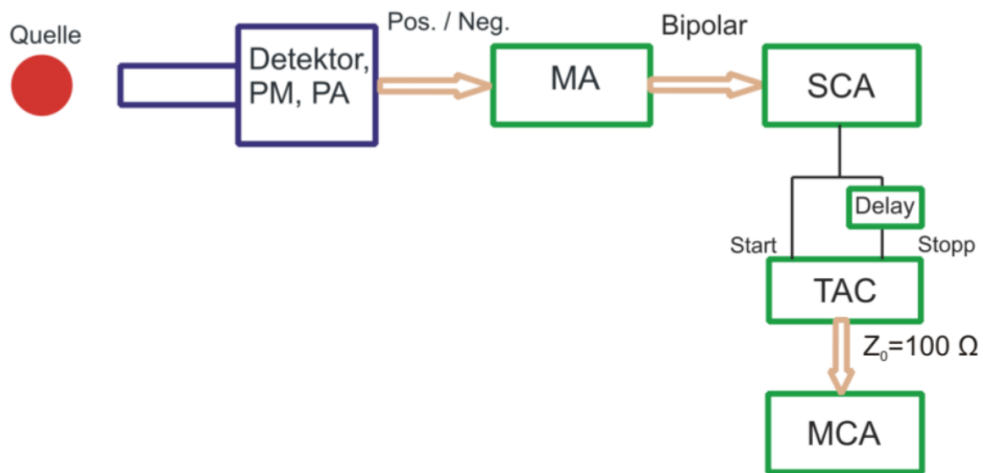


Figure 8: A block circuit diagram for the time calibration.

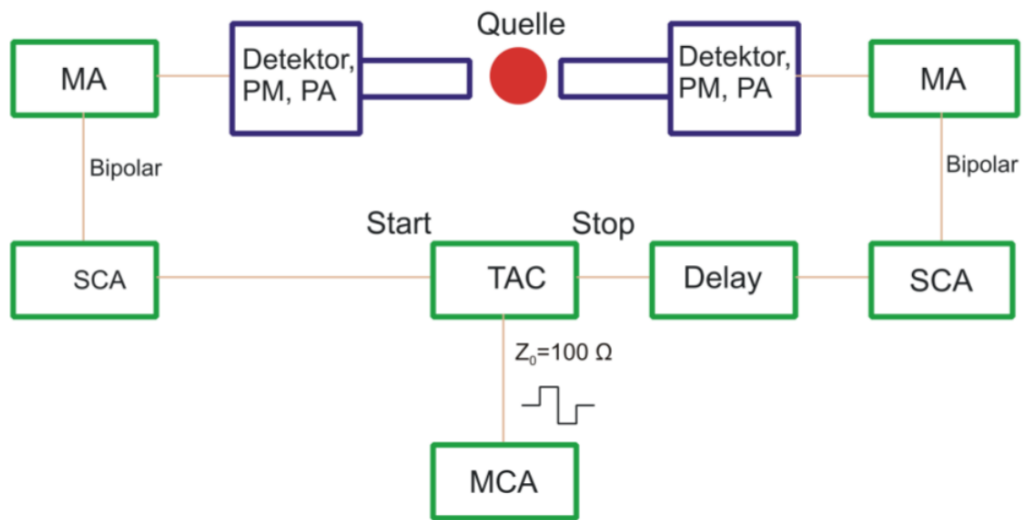
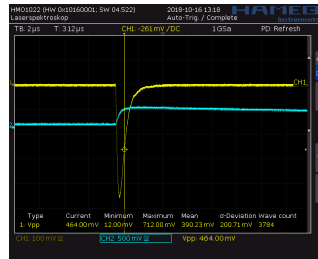


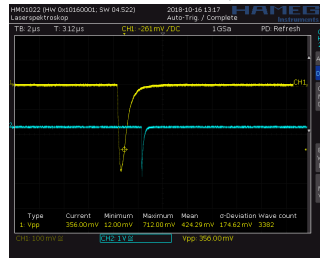
Figure 9: A block circuit diagram for the time calibration.

4 Execution of the Experiment

Firstly we looked at the different signals, the NIM-modules as well as the ones from the pre amplifier and the photo multiplier have as output. Those can be seen in Figure 10. After the pictures were taken, we started with the measurements for every alignment of the samples, starting with the left scintillator with the setup of Figure 7. The measure time was set to 10 minutes. while doing the measurement for the right scintillator, it broke and it took some time to fix it. The technical support noticed a hole inside the scintillator and after round about 7 hours this hole was been covered by duct tape. Because there was not much time left for the measurements, we decided to do the delayed time coincidence measurement right after that. The setup from Figure 9 was set up. We set the amplifier for the TAC so that we could see enough background on the far side of the channels. It was important to place the more active side of the ^{57}Co towards the scintillator which was able to capture the 14.4keV peak. This orientation can be seen in Figure 6b. We started the measurement and saved the data the next morning, like the ones before, on the Computer. The next day, we set the setup from Figure 8 up and did the time calibration, by delaying firstly with 198 ns and did 20ns steps downwards till we reached 7.5 ns.



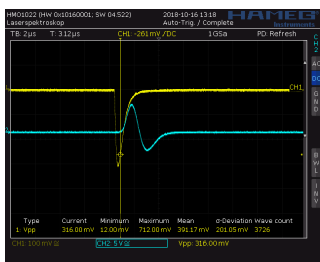
a) Pre amplified signal



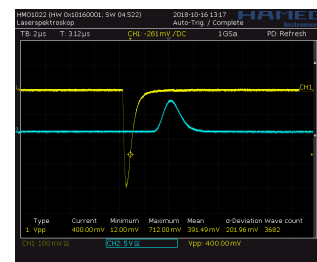
b) Logical negative output from the SCA



c) Logical positive output from the SCA



d) Bipolar output from the MA



e) Unipolar output from the MA

Figure 10: Two signals in comparison the Yellow line is the signal from the photo multiplier, the blue lines are explained in the captions.

5 Data Analysis

5.1 Energy Spectra

In figures 11, 12, 13 and 14, the spectrum of the respective sample, measured with the two different detectors at different orientations, is shown. The two possible orientations of the respective sample are encoded as orientation 1 and 2. The orientations are defined as follows:

Americium: The americium sample has something written on one side (cf. fig. 6a). Therefore we can define the orientation as the relative direction of the marked side to the detector which is taking the respective measurement:

- Orientation 1: Marked side pointing towards detector
- Orientation 2: Marked side pointing away from detector

Cobalt: The two active sides of the cobalt sample are pointing to the left or right side of the sample. In the middle between the two sides the sample has got a yellow label on one side (cf. fig. 6b) and a white label on the other side. We define the orientation by the label which is visible to a person standing in front of the experimental setup, in a way that the orientations specify the direction of the same active side of the sample towards each of the detectors:

- Orientation 1: Yellow label for left detector / white label for right detector
- Orientation 2: White label for left detector / yellow label for right detector

Figures 11, 12, 13 and 14 show the number of counts N for each of the MCA channels. The uncertainty $s_N = \sqrt{N}$ is given by the poisson distribution.

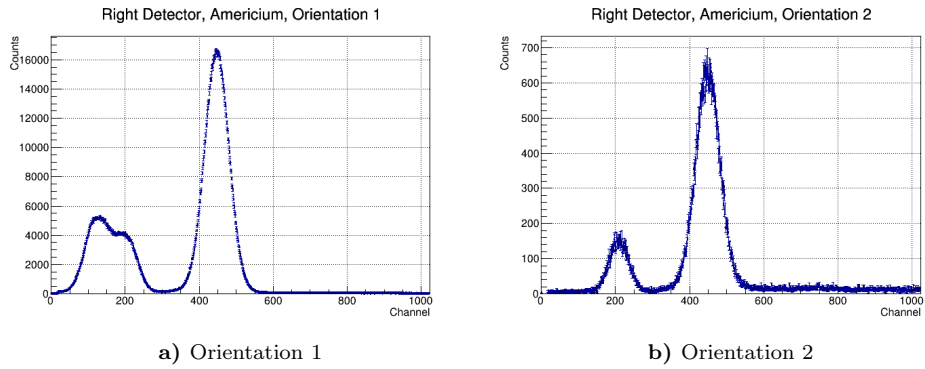


Figure 11: Energy spectrum of ^{241}Am as measured with the detector on the right side at different orientations of the sample

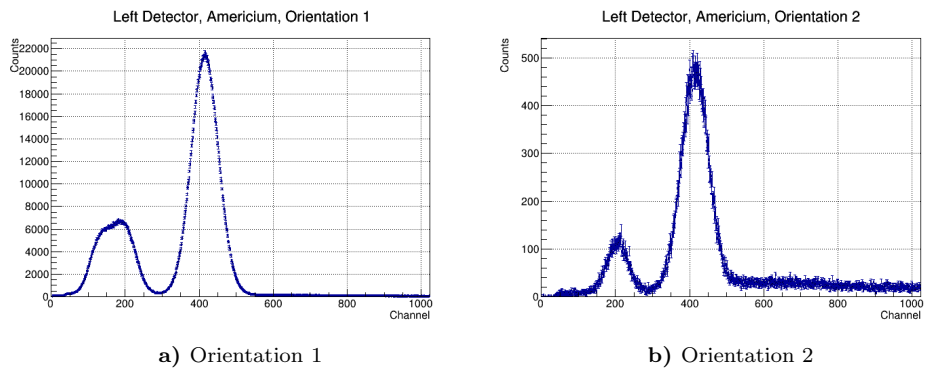


Figure 12: Energy spectrum of ^{241}Am as measured with the detector on the left side at different orientations of the sample

Comparing the four different measurements taken of the ^{241}Am spectrum, it becomes evident that orientation 1 corresponds to the more active side of the sample pointing towards the respective detector and also that the right detector has a better resolution. The two peaks around channels 120 and 200 can only be distinguished in fig. 11a.

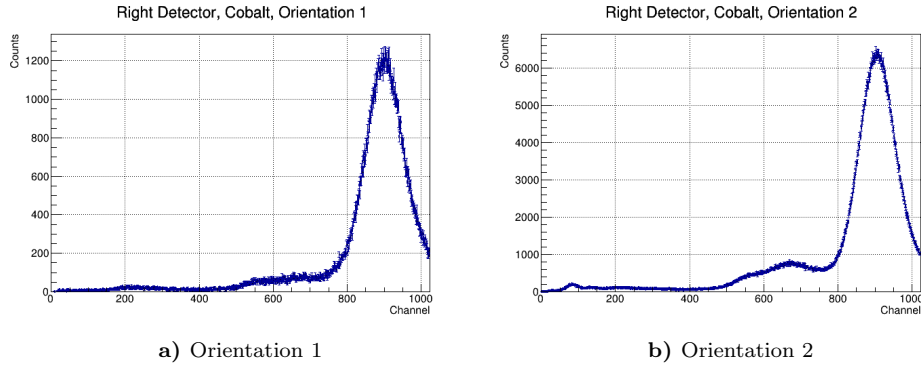


Figure 13: Energy spectrum of ^{57}Co as measured with the detector on the right side at different orientations of the sample

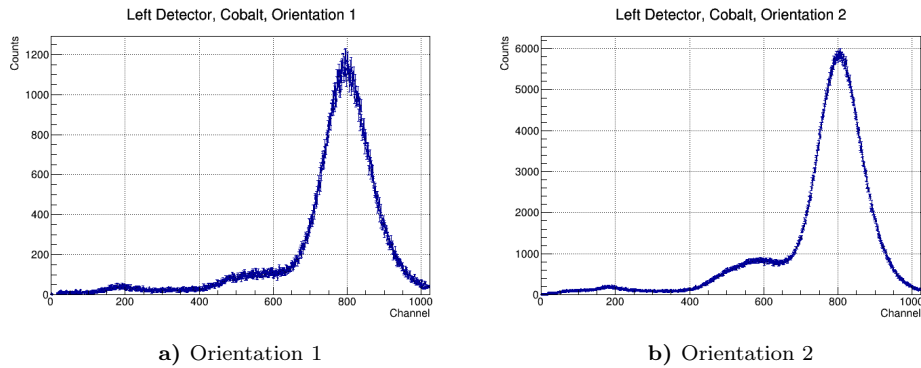


Figure 14: Energy spectrum of ^{57}Co as measured with the detector on the left side at different orientations of the sample

Comparing the four different measurements of the ^{57}Co , it becomes clear that orientation 2 corresponds to the more active side of the sample pointing towards the respective detector. Furthermore, the detector on the right side shows a better resolution. The small peak around channel 90 in fig. 13b is not clearly visible in any other measurement.

5.2 Energy Calibration

Since we need to set the SCA window on the 14.4 keV peak and the 122 keV peak of the ^{57}Co sample (cf. section 4), we first have to relate the MCA channels to their corresponding energies to be able to confirm the correct peaks. For both samples, the detector on the right side showed a better resolution. For this reason, the energy calibration is done with the data obtained from the detector on the right hand side. Of each of the measurements of the ^{241}Am sample in section 5.1, we use the one which shows the clearest resolution, which is the measurement with orientation 1 (fig. 11a). We can identify a peak of high intensity around channel 450 and two peaks of lower intensity around channel 124 and 200. To determine the location of the large peak more exactly, we fit a gaussian function of the form

$$f(x) = a \exp \left[-\frac{(x - \mu)^2}{2\sigma^2} \right] + b \quad , \quad (8)$$

to the data frame around the peak, where the mean value μ is considered as the location of the peak and the standard deviation σ is considered as the uncertainty s_μ . The fit is graphically displayed in fig. 15.

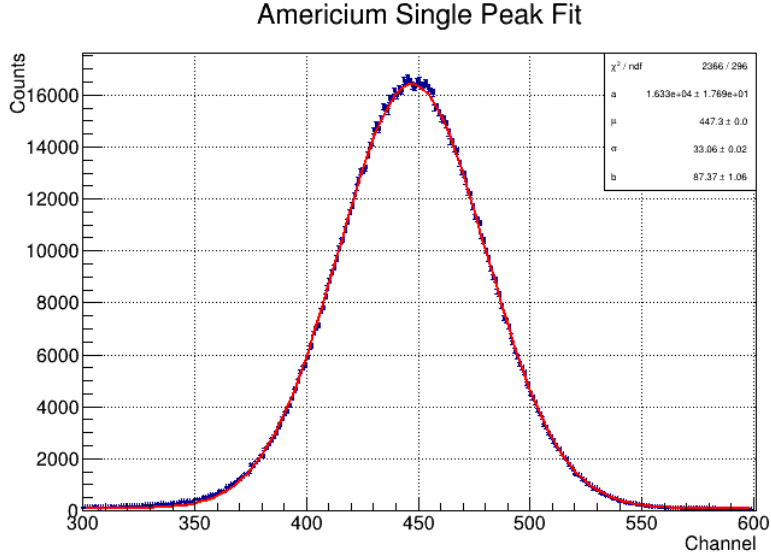


Figure 15: Fit of a gaussian function (eq. 8) to the single peak in the ^{241}Am spectrum

The fit yields the following results for the location of the peak and its uncertainty:

$$\mu = 447.26 \pm 0.03 \quad (9)$$

$$\sigma = 33.06 \pm 0.02 \quad (10)$$

To the two smaller, overlapping peaks, a superposition of two gaussian functions,

$$f(x) = a_1 \exp \left[-\frac{(x - \mu_1)^2}{2\sigma_1^2} \right] + a_2 \exp \left[-\frac{(x - \mu_2)^2}{2\sigma_2^2} \right] + b \quad , \quad (11)$$

is fitted, where μ_1 is considered as the location of the left peak and μ_2 as the location of the right peak. The fit is graphically displayed in fig. 16.

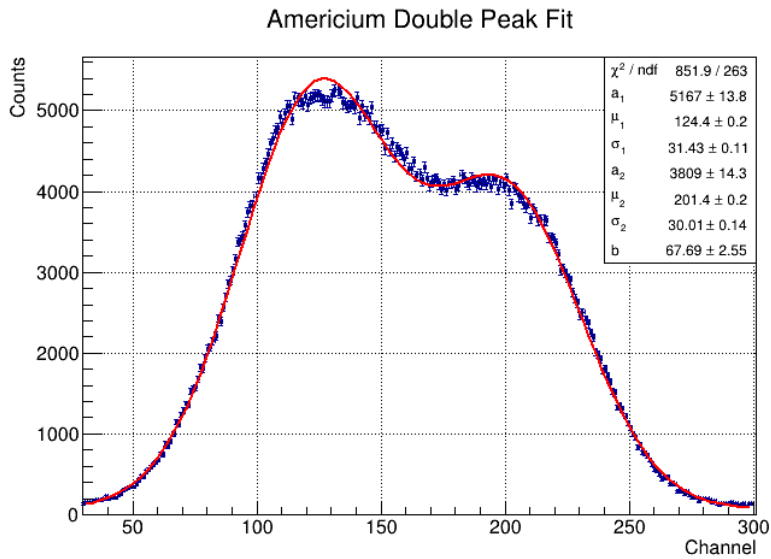


Figure 16: Fit of a superposition of two gaussian functions (eq. 11) to the double peak in the ^{241}Am spectrum

The locations of the two peaks and their respective uncertainties result to:

$$\mu_1 = 124.37 \pm 0.19 \quad (12)$$

$$\sigma_1 = 31.43 \pm 0.11 \quad (13)$$

$$\mu_2 = 201.4 \pm 0.2 \quad (14)$$

$$\sigma_2 = 30.01 \pm 0.14 \quad (15)$$

To identify the peaks in the ^{57}Co spectrum, we again examine the measurement with the highest resolution, which in this case is the one with the right detector and orientation 2. We identify a large peak around channel 900 and a small peak around channel 90. To each of the peaks, a gaussian function (eq. 8) is fitted. The fit to the large peak is displayed in fig. 17:

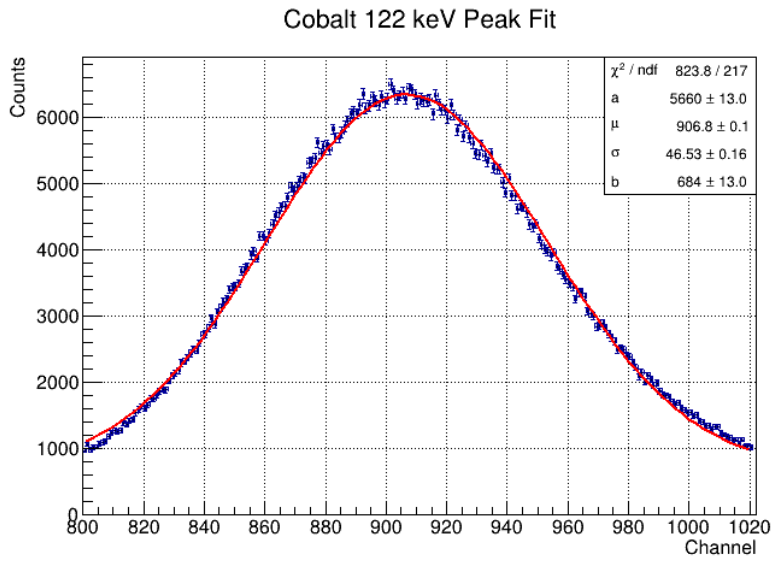


Figure 17: Fit of a gaussian function (eq. 8) to the large peak in the ^{57}Co spectrum

The results for the location and the uncertainty of the large peak are

$$\mu = 906.76 \pm 0.07 \tag{16}$$

$$\sigma = 46.53 \pm 0.16 \tag{17}$$

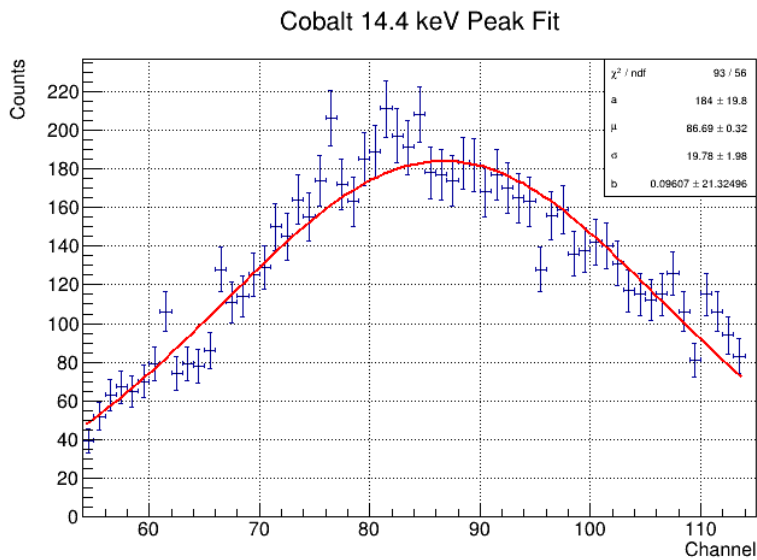


Figure 18: Fit of a gaussian function (eq. 8) to the small peak in the ^{57}Co spectrum

The location and uncertainty of the small peak result to:

$$\mu = 86.7 \pm 0.3 \tag{18}$$

$$\sigma = 19.78 \pm 1.98 \tag{19}$$

We suspect a linear dependence of the photon energy E_γ and the MCA channel. Since a linear fit with only the three known ^{241}Am peaks would not be very meaningful, we also assume the two cobalt peaks to correspond to the energies 14.4 keV and 122.1 keV respectively. The correspondence of the peaks to the energies E_γ given in [1] can be seen in table 1

	Channel	E_γ [keV]
^{241}Am	120 ± 30	26.3
	200 ± 30	33.2
	450 ± 30	59.5
^{57}Co	90 ± 20	14.4
	900 ± 50	122.1

Table 1: Assignment of the peaks found to the Photon energies E_γ given in [1]

A linear function of the form

$$f(x) = mx + c \quad , \quad (20)$$

is fitted to the values shown in table 1. The fit is displayed in fig. 19 .

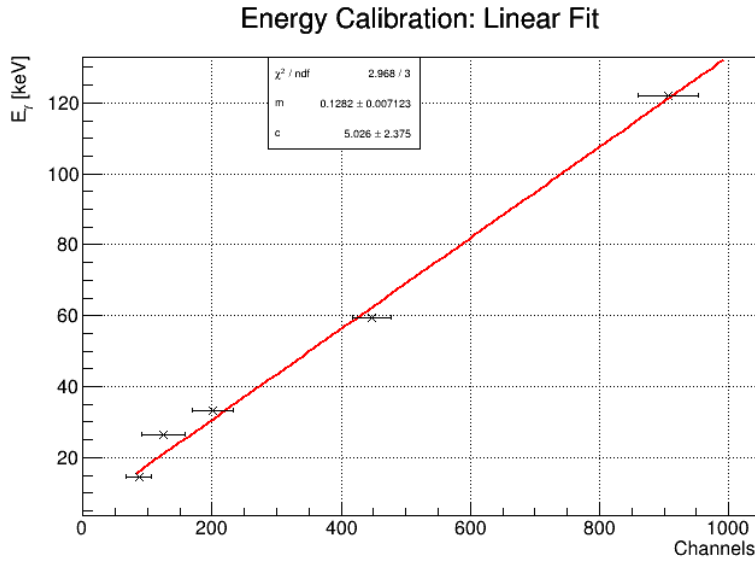


Figure 19: Fit of linear function (eq. 20) for energy calibration

The fit yields the following parameters:

$$m = (0.13274 \pm 0.00002)\text{keV} \quad (21)$$

$$c = (0.6996 \pm 0.0011)\text{keV} \quad (22)$$

With this result, we can check if the assumption we made, that the two visible peaks of ^{57}Co correspond to 14 keV and 122.1 keV respectively, holds. In fig. 19, the linear dependence of the data seems true. To quantify this suspicion, we calculate the Energy E corresponding to the observed peaks and compare them to the literature values E_γ [1]:

	μ []	σ []	E [keV]	s_E [keV]	E_γ	discrepance
^{241}Am	120	30	21	5	26.3	2σ
	200	30	31	5	33.2	1σ
	450	30	62	5	59.5	1σ
^{57}Co	90	20	16	3	14.4	1σ
	900	50	121	9	122.1	1σ

Table 2: Calculation of the energies E corresponding to the observed peaks and comparison to the literature values E_γ

The values in tab. 2 have been calculated with the following formulae:

$$E = m\mu + c \quad (23)$$

$$s_E = \sqrt{m^2\mu^2 \left[\left(\frac{s_m}{m}\right)^2 + \left(\frac{s_\mu}{\mu}\right)^2 \right] + s_c^2} \quad , \quad (24)$$

where it was assumed that the uncertainties s_m , s_c and $s_\mu = \sigma$ are uncorrelated. Since all the peaks correspond to their respective reference values within 1σ (except the 2σ correspondence of the 26.3 keV americium peak), we can hereby verify that the assumptions we made about the peak energies of ^{57}Co were correct. The reduced χ^2 of $\chi_{red}^2 \approx 1.0$ implies the same conclusion since it confirms the linear dependence.

5.3 Time Calibration

The time differences Δt and the respectively responding MCA channels can be found in the lab notes (appendix 7.2). To be able to convert the channels into their corresponding time differences Δt in section 5.4, we plot the MCA channel as a function to the corresponding delay set at the delay unit. Assuming a linear dependence, a function of the form

$$f(x) = ax + b \quad , \quad (25)$$

is fitted to the data. Since for each delay only one channel responded, we assume that there is no error on the channels. Furthermore, the delay is assumed to be exact.

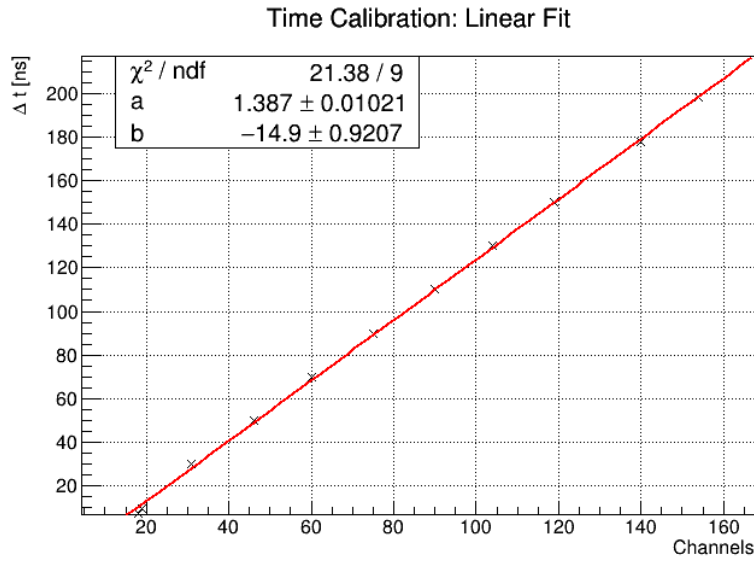


Figure 20: Linear fit relating the MCA channels to their corresponding time difference Δt

The fit results are:

$$a = (1.387 \pm 0.010)\text{ns} \quad (26)$$

$$b = (-14.9 \pm 0.9)\text{ns} \quad (27)$$

5.4 Half Life of the 14.4 keV State of ^{57}Fe

5.4.1 SCA Windows

The SCA window for the respective peaks have been set to be symmetric around the maximum of the peak and to roughly coincide with the standard deviation of the gaussian-shaped peak. The resulting MCA measurements are displayed in fig. 21.

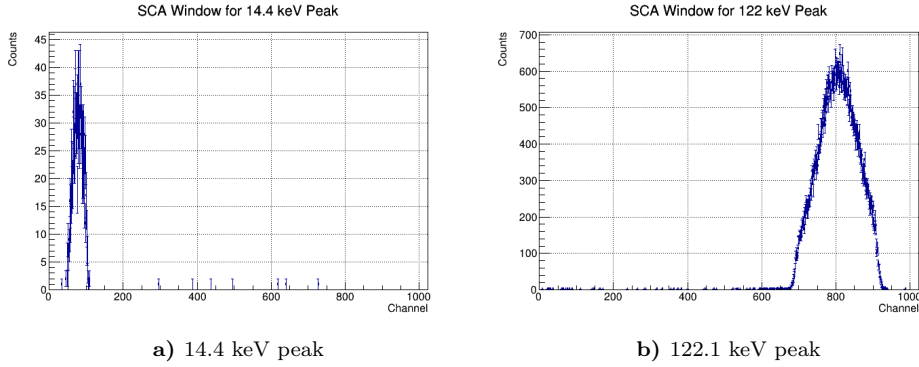


Figure 21: plots of the MCA measurement with the SCA windows set on the respective ^{57}Co peaks

The detector on the left side was used for the 122.1 keV peak and the detector on the right side for the 14.4 keV peak. The values the SCA windows were set to can be found in the lab notes (appendix 7.2). Using the zoom function of the interactive window of the python 2.7 module `matplotlib.pyplot`, we obtain a rough estimation of how the SCA window translates into its corresponding MCA channels. The left and right border of the respective peak in fig. 21 are graphically determined as the channels where the number of counts reaches zero and the respective uncertainty is graphically determined to include statistical fluctuations around this point. The results are shown in table 3.

Detector	Peak	left border [channel]	right border [channel]
left	14.4 keV	48 ± 2	109 ± 2
right	122.1 keV	680 ± 5	925 ± 5

Table 3: Borders of the two peaks used for the delayed coincidences measurement

Since the energy calibration was only done for the detector on the right hand side, we can only determine the corresponding energy window for the 14.4 keV peak. Therefor we use equations 23 and 24, which results in the following energy values for the left and right border of the SCA window for the 14.4 keV peak:

$$E_l = (11 \pm 2)\text{keV} \quad (\text{left border}) \quad (28)$$

$$E_r = (19 \pm 2)\text{keV} \quad (\text{right border}) \quad (29)$$

This corresponds to an energy range of

$$E_r - E_l = (8 \pm 3)\text{keV} \quad . \quad (30)$$

we can calculate half the energy range,

$$\frac{E_r - E_l}{2} = (4.0 \pm 1.4)\text{keV} \quad , \quad (31)$$

and compare it with the statistical uncertainty $s_E = 3 \text{ keV}$ from table 2. They coincide within 1σ which tells us that we set the SCA window correctly.

5.4.2 Delayed Coincidence Measurement

The delayed coincidence measurement was done during a measurement time of 56290.06 s. A plot of the measurement is displayed in fig. 22.

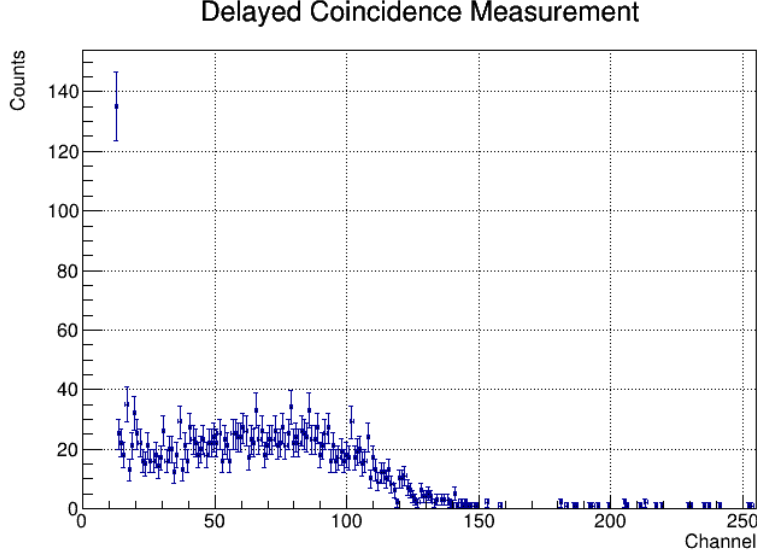


Figure 22: Plot of the delayed coincidence measurement

5.4.3 Random Coincidences

Since one of the detectors was broken for several hours during the experiment, we didn't have enough time to perform a full background measurement. Therefore we calculate the unweighted average of the counts of all channels ≥ 150 and consider the standard deviation of the set as the uncertainty on the number N_B of background counts:

$$N_B = 0.3 \pm 0.5 \quad (32)$$

5.4.4 Linear Fit

Since we expect to find an exponential dependence of the counts N and Δt , according to equation 7,

$$N(\Delta t) = N_0 \exp \left[\frac{\Delta t + t_D}{\tau} \right] ,$$

we can take the logarithm of each of the counts and fit a linear function

$$f(x) = \alpha x + \beta \quad . \quad (33)$$

By comparison of equations 33 and 7, we can calculate the life time τ' with the value α obtained from the fit:

$$\tau' = \frac{1}{\alpha} \quad . \quad (34)$$

τ' is still in units of MCA channels, so with equation 25 and the values a and b obtained in section 5.3, we can calculate the life time τ in ns and therefrom the half-life $T_{1/2}$ of the

14.4 keV state of ^{57}Fe :

$$\tau = a\tau' + b \quad (35)$$

$$T_{1/2} = \tau \log(2) \quad (36)$$

The uncertainties on τ and $T_{1/2}$ are calculated through gaussian error propagation, assuming that a, b and α are uncorrelated:

$$s_\tau = \sqrt{\left(\frac{a}{\alpha}\right)^2 \left[\left(\frac{s_\alpha}{\alpha}\right)^2 + \left(\frac{s_a}{a}\right)^2 \right] + s_b^2} \quad (37)$$

$$s_{T_{1/2}} = s_\tau \log(2) \quad (38)$$

The uncertainties s_a , s_b , and s_α are the statistical uncertainties which result from the respective χ^2 minimization. Through the logarithm, the uncertainties $s_{\log(N)}$ on the counts will become asymmetrical:

$$s_{\log(N),u} = \log(N + s_N) - \log(N) \quad (\text{upper error}) \quad (39)$$

$$s_{\log(N),l} = \log(N) - \log(N - s_N) \quad (\text{lower error}) \quad (40)$$

The calculated values can be found in appendix 7.1.

For the fit, we use the data of channels 23 to 90. Instead of using the log-likelihood method to fit the function to the data, we decided to use the standard χ^2 minimization. The reason for this is that the ROOT class `TGraphAsymmErrors` does not support log-likelihood fitting, while the histogram classes, which do support log-likelihood fitting, don't support asymmetric uncertainties. The $\log(N)$ data obtained and the linear fit are displayed in fig. 23.

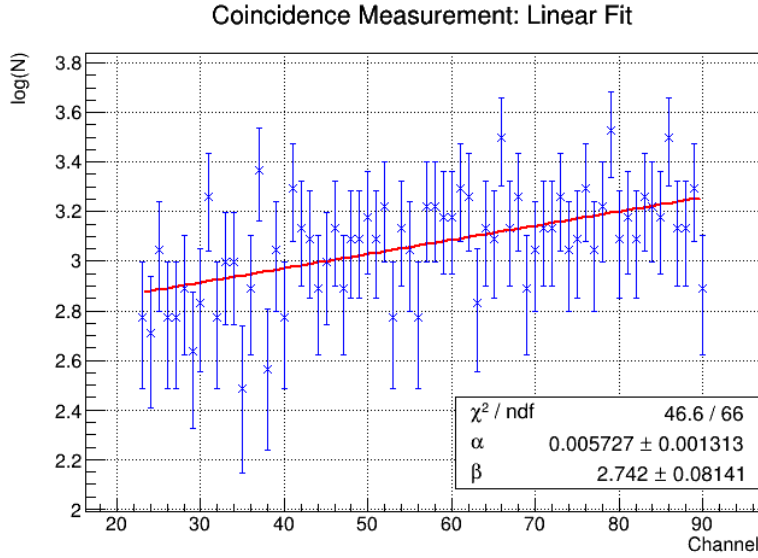


Figure 23: Linear fit (eq. 33) to $\log(N)$ of channels 23 to 90 of fig. 22.

The parameters α and β resulting from the fit are

$$\alpha = (5.7 \pm 1.3) \cdot 10^{-3} \quad (41)$$

$$\beta = 2.74 \pm 0.08 \quad (42)$$

The reduced χ^2 is

$$\chi_{red}^2 \approx 0.7 \quad . \quad (43)$$

From α we calculate, according to equations 35 and 36:

$$\tau = (230 \pm 50)\text{ns} \quad (44)$$

$$T_{1/2} = (160 \pm 40)\text{ns} \quad (45)$$

The relative uncertainty of $T_{1/2}$ is:

$$\frac{s_{T_{1/2}}}{T_{1/2}} = 25\% \quad (46)$$

5.4.5 Exponential Fit

We can directly fit the data of channels 23 to 90 with an exponential function of the form

$$f(x) = \exp[\alpha x + \beta] + c \quad . \quad (47)$$

The initial estimates for the parameters α and β are taken from the linear fit (equations 41 and 42). The initial estimate for the background parameter c is the background N_B (eq. 32). To be able to judge the parameter estimation in comparison to the fit result, the fit function with the estimated parameters is also drawn into the diagram.

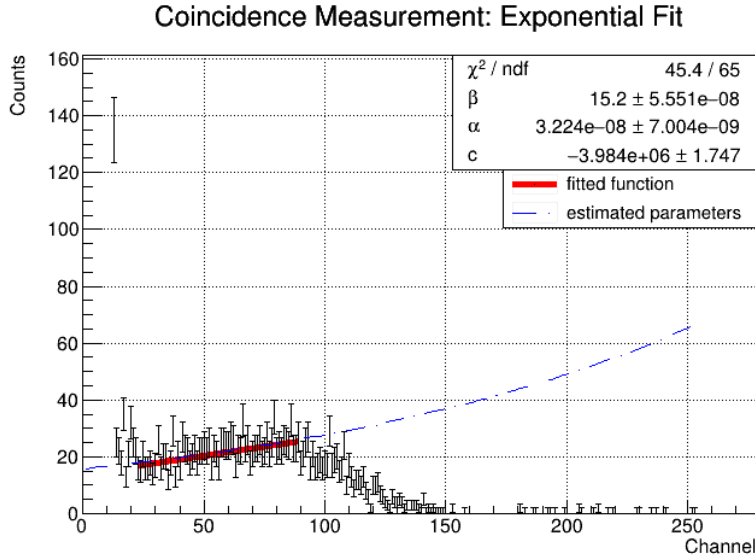


Figure 24: Exponential fit (eq. 47) to the counts N of channels 23 to 90. The function with the estimated parameters is drawn as a blue line.

Although the estimated parameters seem to fit the data well and the fit result shows a good consistency with both the data ($\chi_{red}^2 \approx 0.7$) and the estimated function (graphically), the result for the fit parameters obviously doesn't make physical sense. The background parameter c , which should be around zero, is of order -10^6 and the resulting life time and half life are of order 10 ms. Therefore, instead of determining the global minimum of χ^2 , we have to look for a local minimum by constraining the fit parameters to a range that makes physical sense. We choose the range

$$\xi \in [0, 100] \quad \forall \xi \in \{\alpha, \beta, c\} \quad . \quad (48)$$

The fit with constrained parameters is shown in fig 25.

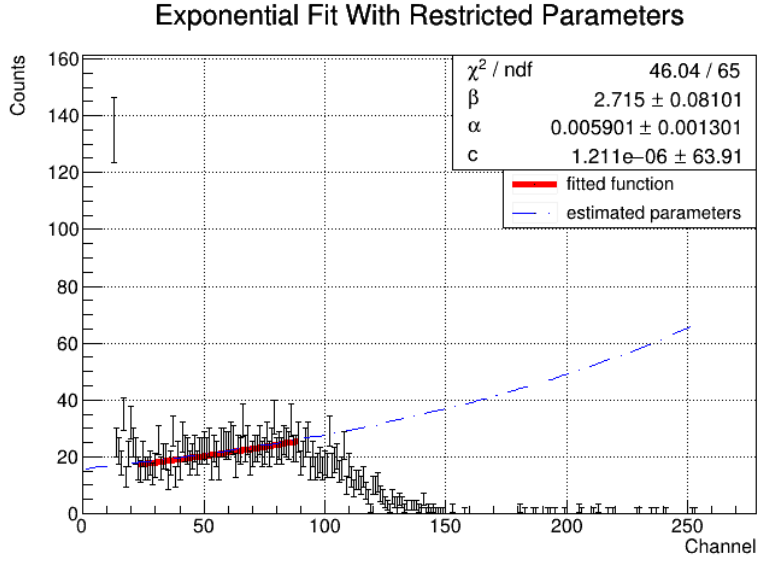


Figure 25: Exponential fit (eq. 47) to the counts N of channels 23 to 90, where the fit parameters are constrained by eq. 48. The function with the estimated parameters is drawn as a blue line.

The fit results are:

$$\alpha = (5.9 \pm 1.3) \cdot 10^{-3} \quad (49)$$

$$\beta = 2.71 \pm 0.08 \quad (50)$$

$$c = 0 \pm 60 \quad (51)$$

The reduced χ^2 ,

$$\chi_{red}^2 \approx 0.7 \quad (52)$$

shows the same goodness of the correlation as the linear fit (fig. 23) and the other exponential fit (fig. 24) which justifies the constraint (eq. 48). With equations 35 and 36, we obtain:

$$\tau = (220 \pm 50)\text{ns} \quad (53)$$

$$T_{1/2} = (150 \pm 40)\text{ns} \quad (54)$$

The relative uncertainty of $T_{1/2}$ is:

$$\frac{s_{T_{1/2}}}{T_{1/2}} = 27\% \quad (55)$$

6 Summary and Discussion of Results

In this experiment, the half life of the 14.4 keV state of ^{57}Fe has been determined by measuring the exponential decay curve with the method of delayed coincidences. The data has been processed by two methods. On one hand, the natural logarithm of the counts N of each MCA channel has been calculated and a linear function has been fitted. On the other hand, the data has directly been fitted with an exponential function. The reference value of $T_{1/2} = 98$ ns is given in the lab guide [1]. The results are:

	$T_{1/2}$ [ns]	consistency
linear fit	160 ± 40	2σ
exponential fit	150 ± 40	2σ

Table 4: Results for the half life $T_{1/2}$ of the 14.4 keV state of ^{57}Fe and consistency with the reference value $T_{1/2} = 98$ ns

Both results coincide within 2σ with the reference value. This is a rather good consistency thanks to the great uncertainties, considering that the data obtained (cf. fig. 22) was not very good for multiple reasons.

Because one of the detectors was broken for several hours during the experiment, we were not able to take a meaningful measurement of random coincidences (background measurement). We calculated the background counts N_B as the average of the counts of all channels ≥ 150 to

$$N_B = 0.3 \pm 0.5 \quad (56)$$

which can only be seen as a rough estimation to the poisson statistics of the counts (obviously, negative counts at the lower error boundary don't make sense). It does, for example, not include a possibly higher distribution of random coincidences towards the first few channels, which would result in a systematically too small α in the fit functions and therefore in systematically too large $T_{1/2}$ values. However, N_B coincides well within 1σ with the background parameter $c = 0 \pm 60$, which, because of its great uncertainty is also just a rough estimation. The high statistical uncertainty does not consider the poisson statistics of counting experiments.

The counts in the exponential range of fig. 22 are rather low, which results in high relative uncertainties. Correspondingly, the measured counts scatter strongly around the expected exponential curve. This results in high relative errors of $T_{1/2}$ of 25% from the linear fit and of 27% from the exponential fit. For low counts, the probability distribution of the counts in each channel is a Poisson distribution which, by the standard procedure of gaussian error propagation, is only approximated by a gaussian distribution. This could result in an overestimation of errors, for example for the background N_B , where negative counts clearly don't make sense. A low count rate can possibly be caused by an SCA window which is set too narrow. In our case, in section 5.4.1, we were able to confirm that the energy range of the SCA window coincides within 1σ with the uncertainty of the peak itself. Thus, a wider SCA window would have likely produced a systematical error due to photons of energies not belonging to the 14.4 keV peak being detected.

The low count rate could possibly have been improved by different settings at the main amplifier and the SCA. Unfortunately, because of the lost time due to the broken detector, we didn't have enough time to take test measurements and try different settings.

7 Appendix

7.1 Calculation of Asymmetric Errors

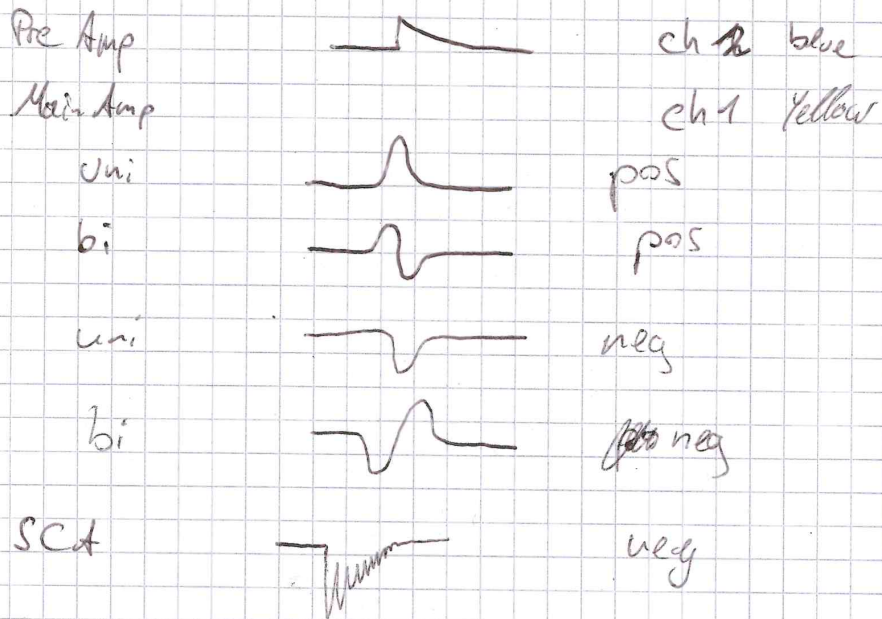
Channel	$\log(N)$ []	lower error []	upper error []	Channel	$\log(N)$ []	lower error []	upper error []
23	2,77	0,29	0,22	57	3,22	0,22	0,18
24	2,71	0,30	0,23	58	3,22	0,22	0,18
25	3,04	0,25	0,20	59	3,18	0,23	0,19
26	2,77	0,29	0,22	60	3,18	0,23	0,19
27	2,77	0,29	0,22	61	3,30	0,21	0,18
28	2,89	0,27	0,21	62	3,26	0,22	0,18
29	2,64	0,31	0,24	63	2,83	0,28	0,22
30	2,83	0,28	0,22	64	3,14	0,23	0,19
31	3,26	0,22	0,18	65	3,09	0,24	0,19
32	2,77	0,29	0,22	66	3,50	0,19	0,16
33	3,00	0,25	0,20	67	3,14	0,23	0,19
34	3,00	0,25	0,20	68	3,26	0,22	0,18
35	2,48	0,34	0,25	69	2,89	0,27	0,21
36	2,89	0,27	0,21	70	3,04	0,25	0,20
37	3,37	0,21	0,17	71	3,14	0,23	0,19
38	2,56	0,32	0,24	72	3,14	0,23	0,19
39	3,04	0,25	0,20	73	3,26	0,22	0,18
40	2,77	0,29	0,22	74	3,04	0,25	0,20
41	3,30	0,21	0,18	75	3,09	0,24	0,19
42	3,14	0,23	0,19	76	3,30	0,21	0,18
43	3,09	0,24	0,19	77	3,04	0,25	0,20
44	2,89	0,27	0,21	78	3,22	0,22	0,18
45	3,00	0,25	0,20	79	3,53	0,19	0,16
46	3,14	0,23	0,19	80	3,09	0,24	0,19
47	2,89	0,27	0,21	81	3,18	0,23	0,19
48	3,09	0,24	0,19	82	3,09	0,24	0,19
49	3,09	0,24	0,19	83	3,26	0,22	0,18
50	3,18	0,23	0,19	84	3,22	0,22	0,18
51	3,09	0,24	0,19	85	3,18	0,23	0,19
52	3,22	0,22	0,18	86	3,50	0,19	0,16
53	2,77	0,29	0,22	87	3,14	0,23	0,19
54	3,14	0,23	0,19	88	3,14	0,23	0,19
55	3,04	0,25	0,20	89	3,30	0,21	0,18
56	2,77	0,29	0,22	90	2,89	0,27	0,21

Table 5: Values of the natural logarithm of the measured Counts and respective upper and lower uncertainties used for fitting.

7.2 Lab Notes

short Half life

Signal shapes



Energy spectrum

Cobalt, left (right MA)

MA Amplifier 1,3 div
 Course Gain 200
 Shaping time 0,6 μ s

SCA Delay 0
 Upper Level 10,1
 Lower Level 0,5

PA 851V 27

Preset 600s

Am links, Ullah rechts. 390.12s

Left scintillator:

Cobalt:

coagelspekti.tka

CO Weisspekt.tka

Americium:

AM links scint klein links.tka

AM links scint klein rechts.tka

Detector (Right scintillator broke) took like 7 hrs to fix. Fixed with gaffa tape

Set SCA for 172 keV Peak:

Delay 0

Upper Level 4,99

Lower Level 3,76

Final energy calib time = 400.12

MA settings right scinti (left ms)

Ampli 4,76

Gain 100

Sh. Time 0.5 μ s

SCA for 14,4 keV Peak:

Upper Level 0,71

Lower Level 0,38

Delay 0,9

Time Calibration

Delay [ns]	Channel
198	154
178 111	740
150	119
130	104
110	90
90 101	75
70	60
50	46
30 ²⁸	31
35 110	19
7,5	18

New Energy spectra (right scintillator)

Amp 4,81

Course Gain 100

Shaping time 0,5 μ s

SEA Window Open

→ Cobalt, two orientations (Yellow/White)

3 New Gelb Re - tka

3 New Weiss Re - tka

→ Americium, two orientations: Marked side left/right

3 New L Re - tka

3 New R Re - tka

Coincidence Measurement coinc. tka

Measurement time: 56290,06s

All good

good work

20/10

10. 10. 2018

K. Bötz

References

- [1] M.Köhler, M.Köhli *Versuchsanleitung Fortgeschrittenen Praktikum Teil I: Kurze Halbwertszeiten*, 11.04.2011
- [2] Picture taken from:
https://en.wikipedia.org/wiki/List_of_Feynman_diagrams#/media/File:Beta_Negative_Decay.svg 19.09.2018 14:00
- [3] Picture taken from:
<https://classconnection.s3.amazonaws.com/815/flashcards/2276815/jpg/elec-capture1356714896919-thumb400.jpg>
- [4] Picture taken from:
http://www.tpub.com/doeinstrument/instrumentation%20and%20control_files/image237.jpg
- [5] Picture taken from :
M.Köhler, M.Köhli *Versuchsanleitung Fortgeschrittenen Praktikum Teil I: Kurze Halbwertszeiten*, 11.04.2011 Who cite: Y.A. Akovali, Nuclear Data Sheets 74, 461 (1995)